First-Principles Study of Monolayer *penta*-CoS_2 as a Promising Anode Material for Li/Na-ion Batteries

M. Debbichi,[1,*] A. Mallah,[2] M. Houcine Dhaou,[3] and S. Lebègue[4]

[1] *Université de Monastir, Faculté des Sciences de Monastir, Laboratoire de la Matière Condensée et Nanosciences LR11ES40, Monastir 5019, Tunisia*

[2] *Department of Chemistry, College of Science, Qassim University, P.O. Box 6644, Buraydah Almolaydah, Buraydah 51452, Saudi Arabia*

[3] *Department of Physics College of Science, Qassim University Buraydah, Almolaydah 51452-P.O. Box 6644, Saudi Arabia*

[4] *Université de Lorraine, LPCT, CNRS, UMR 7019, BP 70239, Vandoeuvre-lès-Nancy Cedex, 54506, France*

(Received 29 March 2021; revised 8 June 2021; accepted 26 July 2021; published 10 August 2021)

Using first-principles calculations, we investigate the properties of the CoS_2 monolayer pentagonal structure as a possible anode material for Li- and Na-ion batteries. The geometrical optimization reveals that the metal atom prefers to be adsorbed on the hollow site, and that the diffusion barrier of Li and Na can be as low as 0.22 eV, which would allow a relatively fast diffusion on the surface. Moreover, our calculations demonstrate that the CoS_2 monolayer has a theoretical specific capacity of 653.31 and 326.77 mAh g^{-1} for Li and Na, respectively, which in the case of Li is larger than the capacity of other two-dimensional materials used as an anode material. Overall, the CoS_2 monolayer in this structure shows excellent electrochemical properties, making it a promising candidate for use as the anode material in metal-ion batteries.

DOI: 10.1103/PhysRevApplied.16.024016

I. INTRODUCTION

The environmental pollution and the increasing energy demand have pushed researchers to replace dwindling supplies of fossil fuels by developing high-performance energy-storage devices [1]. Therefore it is urgent to popularize and explore renewable energy sources with high performances in term of high-energy density, high-power density, and long cycling life. Rechargeable ion batteries are alleged to have an enormous potential, given their attractive performances of high energy density, rational working voltage, and good cyclability [1–3]. So far, a variety of systems have been explored, including lithium-ion batteries (LIBs), sodium-ion batteries (SIBs), etc. Although the performance of these batteries have largely improved in the past years, their further development is still limited [4]. Recently, considerable effort has been made to improve their performance by developing electrode materials [4,5]. The required electrode materials must not only have high electrical and thermal conductivities, but also need to have a sufficiently high strength, hardness, and heat resistance [6].

At present, considerable effort has been made to develop cathode materials with large interstitial space. Recently and since the discovery of graphene [7], two-dimensional (2D) materials have emerged in various research fields with a wide range of applications from electronic devices [8–11], including energy-storage technologies such as batteries [4–6,12–16]. This is due to the excellent characteristics of their surfaces, which permits a fast ion diffusion and large ionic insertion channels, compared to bulk materials and other dimensional nanomaterials [17]. Numerous 2D materials have been reported as potential electrodes for energy-storage applications: for example, transition metal dichalcogenides (TMDCs) [4], transition metal carbides and nitrides (MXenes) [18–20], and transition metal oxides [21,22]. Among these, transition-metal sulfides are known to be potential candidates for anode materials due to their high theoretical capacity, versatile material types, sufficient abundance, cost effectiveness, and robust structures [4,23]. For instance, the potential of VS_2 monolayers has been demonstrated by first-principles calculations as the electrode material for Li-, K-, Mg-, and Al-ion batteries with theoretical capacities of 1397, 1863, 466, and 78 mA h g^{-1}, respectively, and a diffusion barrier of less than 0.4 eV [18]. Also, XS_2(X = Mo, Nb, Zr, and Ti) are found to have a suitable open-circuit voltage range as a Na anode material (0.49–0.95 V versus Na^+/Na), with theoretical capacities of 260–339 mA h g^{-1}. These materials also showed Na ion migration barriers as low as 0.22 (TiS_2)

*mourad_fsm@yahoo.fr

 © 2021 American Physical Society

and 0.07 eV (NbS_2) [24]. Moreover, Veenu *et al.* [25] performed first-principles calculations of Li adsorption on a Mo_2CS_2 monolayer and predicted a diffusion barrier of 0.24 eV. They also showed that Mo_2CS_2 has a large storage capacity (410 mA h g^{-1}), larger than some available electrode materials such as graphite, MoS_2, TiO_2, Ti_3C_2, and Mn_2CF_2. Also tin (Sn)-based sulfides SnS and SnS_2 materials are considered as promising anode materials for LIBs and NIBs due to their high theoretical capacities [(1137 mA h g^{-1} for LIBs and 1022 mA h g^{-1} for NIBs) and (1231 mA h g^{-1} for LIBs and 1136 mA h g^{-1} for NIBs), respectively] [26].

Cobalt is a popular metal within material science: cobalt-based materials have attracted much attention in many fields like energy storage [27], especially for Li and Na batteries [5,6]. Among them, cobalt sulfides have emerged as promising semiconductor materials and possess a wide range of applications like supercapacitors, dye-sensitized solar cells, and lithium- and sodium-ion batteries [28]. Cobalt sulfides with many phases and different stoichiometry coefficients, including CoS, CoS_2, Co_4S_3, and Co_8S_9 have attracted increasing attention due to their electrochemical performance (high first-cycle efficiency and a high theoretical capacity) [29–31]. Motivated by the excellent properties of CoS_2-based electrode (high capacity, lower over potential, and better cycling stability) compared with other sulfide materials [32], and the advantages of this allotrope pentagonal structure, which is found to be mainly responsible for the high Li/Na ion-storage capacity and the fast diffusivity [33], we study, by density functional theory (DFT), the adsorption, diffusion behavior, and electrochemical performance of metal ion adsorbed in CoS_2-pentagonal Cairo-tiled structures.

II. COMPUTATIONAL DETAILS AND METHODS

Our calculations are performed using density functional theory as implemented in the Quantum Espresso package [34]. We choose the projector-augmented-wave (PAW) method for the basis set [35]. The exchange-correlation functional is treated by the Perdew-Burke-Ernzerhof (PBE) [36] form of the generalized gradient approximation (GGA). The energy cutoff of the plane waves is set to 550 eV and the vacuum spacing between two layers is set to 20 Å in order to avoid unwanted interactions between periodic images of the layers. The Brillouin zone (BZ) is integrated using a $12 \times 12 \times 1$ Γ-centered Monkhorst-Pack k-mesh method during the relaxation [37]. The convergence criterion is set to 10^{-6} eV/cell in energy and 10^{-3} eV/Å in forces. To treat the d orbitals of the Co atoms, we adopt the GGA+U approach formulated by Cococcioni *et al.* [38]. The effective U parameter U_{eff} is set to 3.32 eV, consistently with a previous work [39]. For the calculation of the electronic structure, the Brillouin zone is sampled with a k-point grid of $20 \times 20 \times 1$. The climbing image nudged-elastic-band (CI NEB) method [40] is used to calculate the potential energy-diffusion pathway and the minimum diffusion energy barrier of the Li/Na ions on the CoS_2 monolayer. Also a Bader charge analysis is carried out to study the charge distribution and transfer [41].

TABLE I. Calculated structural parameters (a and b in Å), magnetic moment of Co atom m in Bohr magneton, band gap (eV) and relative energy ΔE in meV/unit cell of the CoS_2 monolayer for the nonmagnetic (NM), and the different magnetic configurations (FM, AFM).

Configuration	a	b	m	ΔE	E_g
NM	5.381	5.382	00	678	Metal
FM	5.337	5.431	1.107	34.00	1.19[a],1.96[b]
AFM	5.337	5.432	1.192	00	1.06

[a]Spin-up component.
[b]Spin-down component.

III. RESULTS AND DISCUSSION

A. Structure and electronic properties of CoS_2 monolayers

The CoS_2 monolayer displays a buckled pentagonal structure with the space group $P2_1/c$, where each pentagon is formed by two Co atoms and three S atoms. Each Co atom adopts a planar tetracoordination with four S atoms, forming a pentagonal ring network known as the Cairo pentagonal tiling, as shown in Fig. 1. For the structural optimization of the CoS_2 monolayer, both spin and non-spin polarized solutions are considered, and the results are given in Table I. It is found that the AFM structure has the lowest total energy with in-plane lattice constants (a = 5.337 Å, b = 5.432 Å), which agree well with the parameters reported by Lei *et al.* [39]. In addition, our calculated localized magnetic moments for each Co ion ($1.19\mu_B$) and band-gap energy (1.06 eV) also coincide with earlier theoretical results given by Lei *et al.* [39]. The computed band structure and projected density of states (PDOS) of a CoS_2 monolayer are shown in Fig. 2. It can be seen that the CoS_2 monolayer is a semiconductor with an indirect band gap (X-M) of 1.06 eV.

B. Li/Na adsorption on CoS_2

In order to examine the Li/Na-adsorption capability of the CoS_2 monolayer, which is the prerequisite for using it as an electrode material in Li/Na batteries, we investigate the different lithium and sodium adsorption sites on CoS_2. Three possible adsorption sites are examined, as shown in Fig. 1: (1) the top of a Co atom (site $T1$), (2) the top of a S atom (site $T2$), and the hollow sites above the center of the

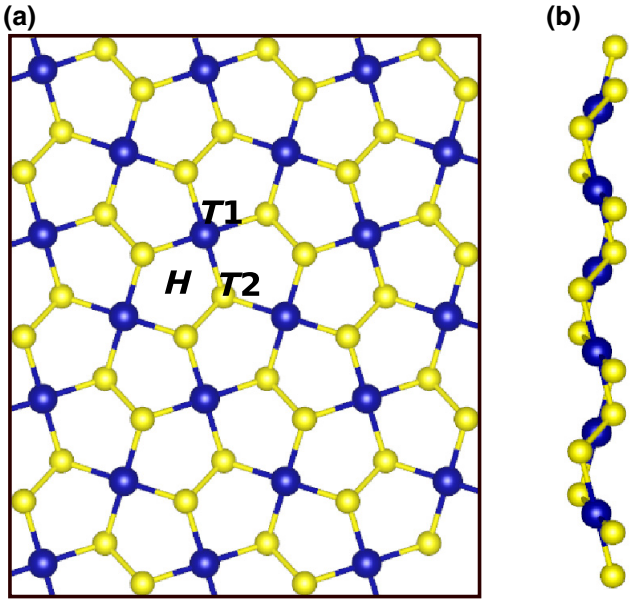

FIG. 1. (a) Top and (b) side views of the optimized $3 \times 3 \times 1$ CoS_2 monolayer. H, $T1$, and $T2$ represent three possible adsorption sites for the adatoms. The cobalt and sulfur atoms are shown with blue and yellow spheres, respectively.

pentagon (site H). We perform a full structural optimization for all the adsorption sites under both spin and nonspin polarized conditions, and a $2 \times 2 \times 1$ supercell of CoS_2 is used in our calculations. The most favorable adsorption site is identified by calculating the adsorption energy using the following equation:

$$E_{\mathrm{ad}} = E(\mathrm{MCoS_2}) - E(\mathrm{CoS_2}) - E(M), \qquad (1)$$

where $E(\mathrm{MCoS_2})$, $E(\mathrm{CoS_2})$, and $E(M)$ are the total energies per atom of CoS_2 with the M adsorbate, pristine CoS_2, and the bulk metal atom, respectively.

According to Eq. (1), a negative adsorption energy represents an exothermic reaction and a strong attractive

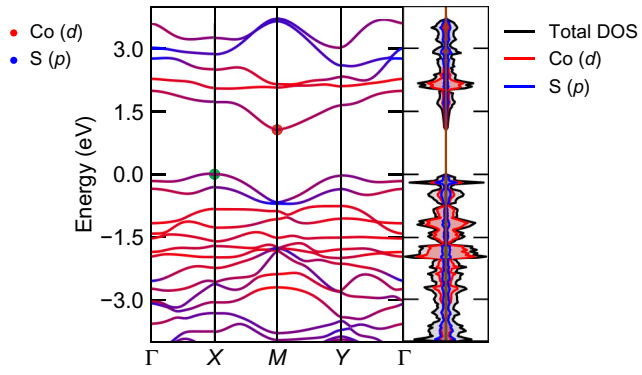

FIG. 2. Orbital-resolved band structure and PDOS of a CoS_2 monolayer.

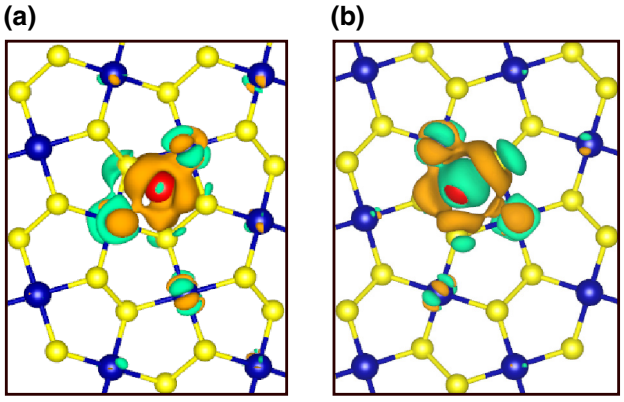

FIG. 3. Charge-density difference of (a) Li atom adsorption and (b) Na atom adsorption on the CoS_2 monolayer with an isovalue of 0.005 e/Å^3. The orange and light green isosurfaces represent the electron accumulation and depletion, respectively.

interaction occurs between the adsorbate and the substrate, which indicates that this system is potentially a suitable cathode material for Li/Na-ion batteries. Our results suggest that all the above metal atoms prefer to be adsorbed above the hollow site, and the corresponding adsorption energies are -211 and -198 meV for Li and Na, respectively.

Moreover, to understand the adsorption behavior of Li/Na ions on the monolayer, the three-dimensional charge-density difference of metal/CoS_2 is shown in Fig. 3, which is obtained as the difference between the valence charge density before and after bonding using the following equation:

$$\Delta\rho = \rho_{\mathrm{CoS2Li/Na}} - \rho_{\mathrm{CoS2}} - \rho_{\mathrm{Li/Na}}, \qquad (2)$$

where $\rho_{\mathrm{CoS2Li/Na}}$ and ρ_{CoS2} denote the total electron densities of the relaxed CoS_2 monolayer with and without metal atoms, respectively, and $\rho_{\mathrm{Li/Na}}$ is the total electron density of the isolated metal atom. In Fig. 3, the orange and light green areas represent the electron accumulation and depletion zones, respectively, and it is found that the metal atoms behave as charge donors. Then a Bader analysis is performed to quantify the charge transfer by using a $250 \times 250 \times 400$ grid for the electron density. It is found that approximately $0.93e$ and $0.89e$ are transferred to the substrate from the adatoms Li and Na, respectively, implying that the Li interacts more strongly with CoS_2 than Na. These findings are in accordance with the value of the adsorption energy.

To further understand the interaction between the metal atom and the CoS_2 monolayer, we calculate the electronic structure of the resultant compound. Figure 4 shows the computed PDOS for these metal-adsorbed systems. It is seen that the CoS_2 monolayer becomes metallic after the adsorption. This transition from a semiconductor to a metal

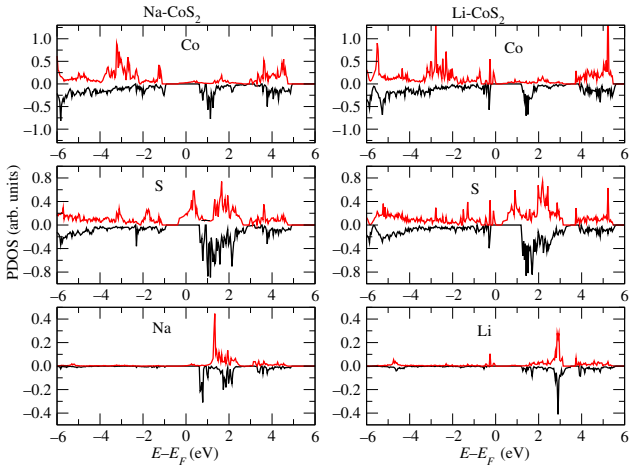

FIG. 4. PDOS when the Li and Na atoms are adsorbed on the CoS_2 monolayer.

is due to the charge transfer from the adatoms to CoS_2. This metallic behavior ensures a good electrical conductivity, which is a desired condition for a battery electrode candidate. The same phenomenon has also been observed in other 2D semiconducting electrode materials such as GaN [42], PC [43], and MX (M = Ge, Sn; X = S, Se) [44].

C. Ion diffusion pathway and energy barrier

The value of the energy barrier represents a useful parameter to evaluate the charge and discharge rates of a rechargeable battery. The calculated diffusion pathway from one stable site to the neighboring stable site is obtained by taking nine images through the diffusion pathways on a $3 \times 3 \times 1$ supercell of the CoS_2 monolayer. The structures of all images are relaxed with a force convergence criterion set up to 10^{-3} eV/Å.

The energy barrier E_b is calculated as the energy difference between the transition state (E_{TS}) and the initial state (E_{IS}): $E_b = E_{TS}$-E_{IS}. In our case, two possible diffusion pathways are considered between two neighboring adsorption sites, denoted as P1(H $\mapsto$ H) and P2(H $\mapsto$ T2 $\mapsto$ H). The corresponding diffusion energy profiles along the optimized pathway for the two metal atoms (Li, Na) are shown in Fig. 5. The nonsymmetrical energy barrier is due to numerical inaccuracies. For the two systems, P1 is the most favorable diffusion pathway, which possesses the lowest diffusion barrier, that is 0.15 eV for Na and 0.21 eV for Li. These barrier values are comparable to that of VS_2 (0.22 eV) [45] and B_2S [46], and lower than typical 2D anode materials, such as graphene (0.31 eV) [47], MoC_2 (0.266 eV) [48], borophene (0.60 eV) [49], MoN_2 (0.78 eV) [50], Mo_2CS_2 (0.24 eV) and other functionalized MXenes $Ti_3C_2F_2$(0.36 eV), $Ti_3C_2(OH)_2$ (0.90 eV) [25].

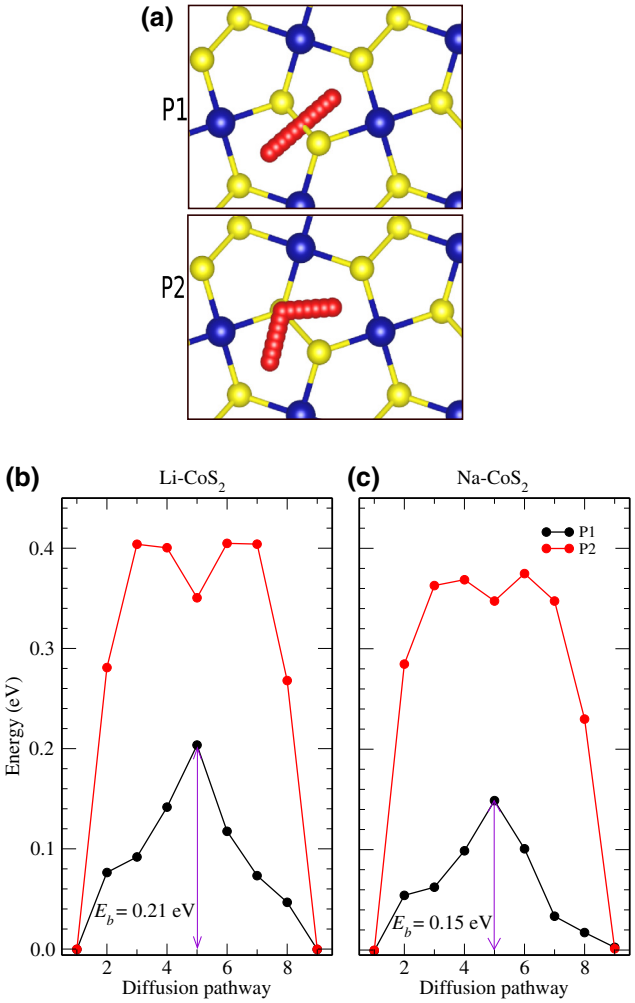

FIG. 5. (a) Top view of the two possible migration paths of Na and Li on the CoS_2 monolayer and (b) the corresponding diffusion barrier profiles.

The diffusion coefficient of the metal atoms on the CoS_2 monolayer can be also evaluated on the basis of transition state theory. By neglecting the change in vibrational free energy, the diffusion coefficient (D) can be calculated by [51,52]

$$D = d^2\omega/\exp\left(\frac{E_a}{k_B T}\right), \tag{3}$$

where d is the diffusion distance, E_a is the activation energy of the diffusion, k_B is Boltzmann's constant, T is the absolute temperature, and ω is the attempt frequency with ω taken as 10^{13} Hz [51,53]. According to our calculations, the diffusion coefficient at 300 K for Li and Na on the CoS_2 monolayer is 2.9×10^{-6} and 3.13×10^{-5} cm^2/s, respectively. Because of the relatively smaller activation energy of the Na atom compared to the Li atom on CoS_2 monolayer, the diffusion is predicted to be faster

in $NaCoS_2$ at room temperature. Our calculated diffusion coefficients are in qualitative agreement with the one for the Na/Li-Nb_2S_2C monolayer [54], Na/Li-TiSSe [51] and larger than that of graphene, C_2N and C_2N/graphene [52,54].

D. Open-circuit voltage and storage capacity of Li and Na on the CoS_2 monolayer

The storage capacity and open-circuit voltage are two helpful parameters for the performance of electrode materials. We increase the number of adsorbed metal atoms on the CoS_2 monolayer in the $2 \times 2 \times 1$ supercell by constructing a series of configurations with the chemical stoichiometry M_xCoS_2. Here, the different numbers of metal atoms are placed on both sides of the CoS_2 monolayer. Firstly, we begin by adding the metal atom one by one on the side of the most stable site to form the first layer, when the sites are occupied on this side, we follow on the other side of the CoS_2 to form the second layer. After the complete occupation of stable sites of the CoS_2 monolayer, the adsorption will occur on the top of the next stable site to form the third and fourth layers of adsorption etc., as shown in Fig. 6(a). For each structure, the ground state is obtained after testing all possible adsorption sites into consideration.

The charge-discharge processes can be described by the following chemical reaction:

$$M_xCoS_2 \Leftrightarrow CoS_2 + xM^+ + xe^-. \tag{4}$$

The open-circuit voltage can be obtained by computing the total energies before and after Li/Na intercalation. To obtain accurate energy values, both the lattice parameters and atomic positions are fully relaxed for the intercalated configurations. By neglecting the volume and entropy effects, the open-circuit voltage (OCV) can be estimated by [55,56]

$$\mathrm{OCV} \simeq \frac{E(CoS_2) + xE(M) - E(M_xCoS_2)}{xe}, \tag{5}$$

where $E(M_xCoS_2)$, $E(CoS_2)$, and $E(M)$ are the total energies of CoS_2 with the M adsorbate, pristine CoS_2, and bulk metal atom, respectively.

The plot of the voltage and metal atoms' content are depicted in Fig. 6(b). It is seen that the OCV gradually decreases with the increase of the number of adsorbed metal atoms because of the enhanced repulsion among metal cations. The evolution of the OCV exhibits two effective plateaus corresponding to the first and second layers of sodium adsorptions. However, for Li adsorption, there are three plateaus. The positive OCV demonstrates that the accommodation of one-layer metal atoms on the CoS_2 monolayer is energetically favorable for both Na and Li metals. For the second layer, the accommodation

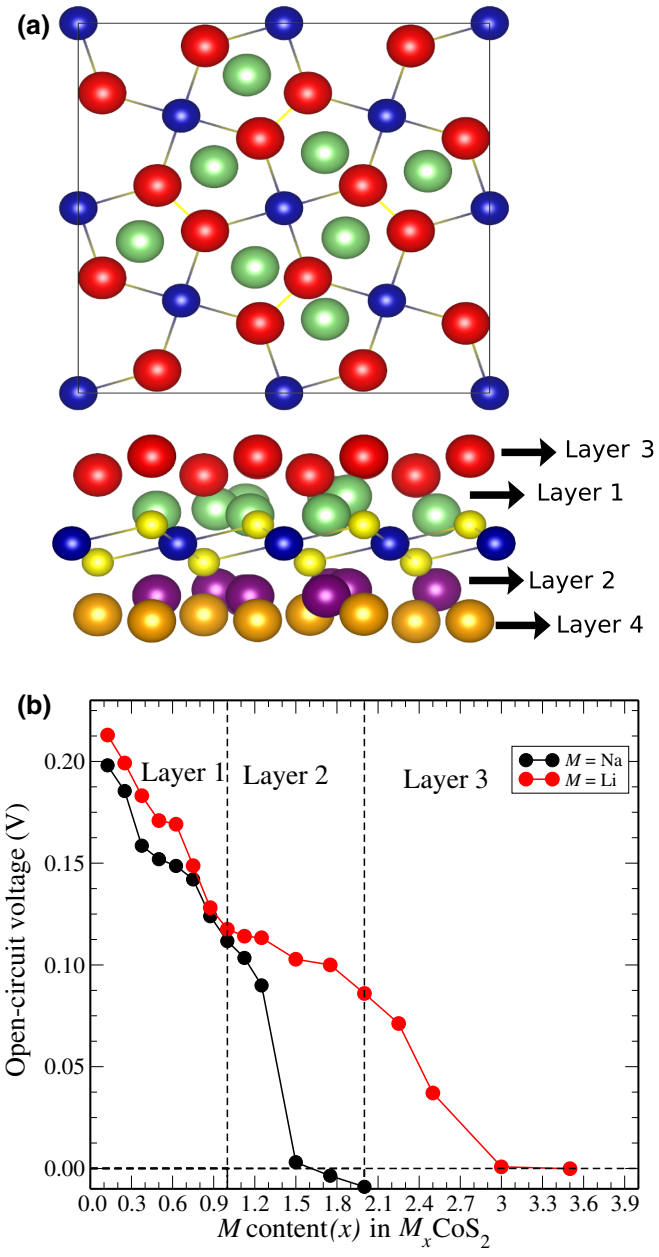

FIG. 6. (a) The top and side view configurations of the adsorbed metal layer on CoS_2 monolayer. (b) The OCV profile with metal ions adsorbed. The red, green, purple, and golden rod represent the metal.

of Li is still energetically favorable, however, the adsorption of Na atoms becomes unstable when x is larger than 1.5, owing to the strong repulsive interaction caused by the Na cations. The corresponding chemical stoichiometry are Li_3CoS_2 and $Na_{1.5}CoS_2$ with an average OCV in the range of 0.0–1.0 V. These values are comparable to some typical electrode materials such as Mo_2C, MoC_2, MoC, Nb_2C, MoN_2, and Ti_3C_4 [48,50], demonstrating the feasibility of a monolayer of CoS_2 as a 2D anode for rechargeable ion batteries.

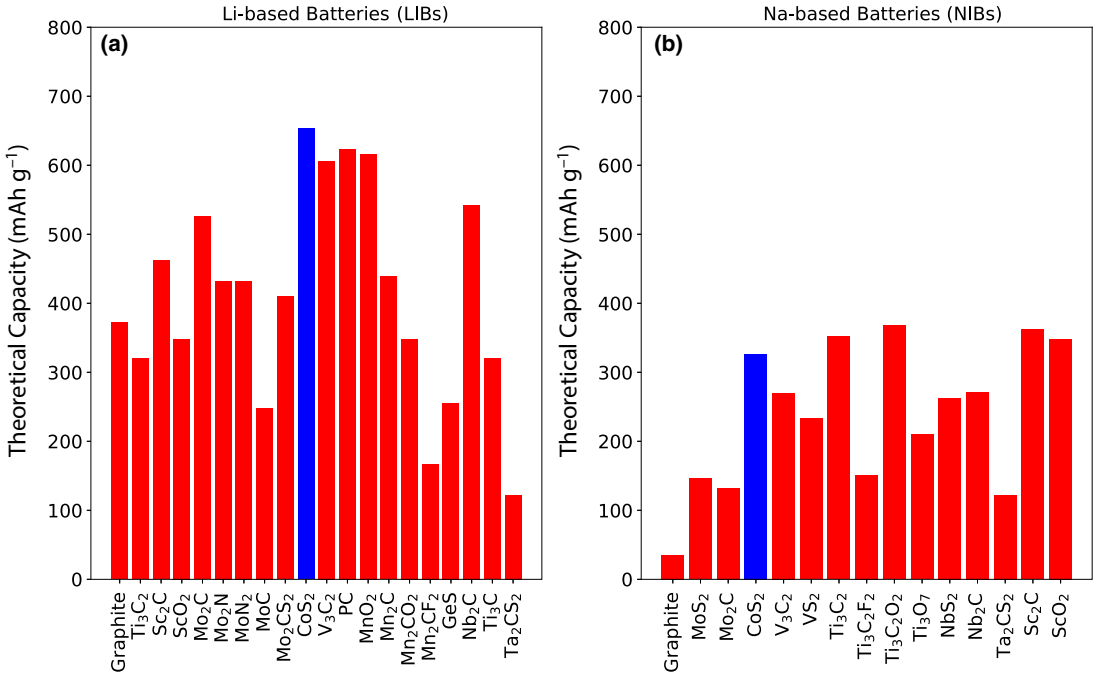

FIG. 7. Comparison of the theoretical capacity of Li/$NaCoS_2$(blue bar) with some selected 2D material-based electrodes for SIBs and LIBs(red bar). The values are taken from Refs. [4,5,21,25,43,45,47,50,51,57–61].

The specific capacity can be estimated as

$$C = \frac{xF}{m}. \tag{6}$$

Here m is the molecular weight of CoS_2 (123.065 g mol^{-1}), F is the Faraday constant (26.8 A h mol^{-1}), and x is the highest concentration of M ion in M_xCoS_2. The obtained maximum capacity of Li and Na are 653.31 and 326.77 mA h g^{-1}, respectively. For comparison the Li and Na storage capacities for several 2D-based structures are illustrated in Fig. 7: our calculated value for $LiCoS_2$ is larger than those of some other predicted 2D electrode materials, while for $NaCoS_2$, our calculated value is larger than most of the other known compounds but lower than the one of Sc_2C, Ti_3C_2, and $Ti_3C_2O_2$.

E. Conclusion

In summary, using density functional theory, we study the structural, electronic, and electrochemical properties of the CoS_2 monolayer in the pentagonal structure. We find that the metal atoms (Li or Na) prefer to absorb on the hollow site, and that this adsorption is accompanied by a large charge transfer to the CoS_2 monolayer, which becomes metallic, ensuring a good electronic conductivity. Then using the CI NEB method, the value of the migration energy barriers on the CoS_2 monolayer is found to be suitable for its use as the anode material in LIBs and NIBs. Furthermore, the specific storage capacity is found to be 653.31 and 326.77 mAh g^{-1} for Li and Na, respectively, which is in the case of Li, much larger than that of other 2D materials used as anodes. Overall, our results suggest that this allotrope of CoS_2 is a very promising compound to be used as the anode in Li-ion batteries. We hope that our work will stimulate further theoretical and experimental researches on this compound.

[1] B. Li, P. Gu, Y. Feng, G. Zhang, K. Huang, H. Xue, and H. Pang, Energy storage: Ultrathin nickel-cobalt phosphate 2D nanosheets for electrochemical Energy storage under aqueous/Solid-state electrolyte, Adv. Funct. Mater. **27**, 1605784 (2017).

[2] H. Fan, H. Yu, Y. Zhang, J. Guo, Z. Wang, H. Wang, N. Zhao, Y. Zheng, C. Du, and Z. Dai, 1D to 3D hierarchical iron selenide hollow nanocubes assembled from $FeSe_2$@C core-shell nanorods for advanced sodium ion batteries, Energy Storage Mater. **10**, 48 (2018).

[3] B. Dunn, H. Kamath, and J.-M. Tarascon, Electrical energy storage for the grid: A battery of choices, Science **334**, 928 (2011).

[4] Y. Zhang, L. Zhang, T.'a. Lv, P. K. Chu, and K. Huo, Two-dimensional transition metal chalcogenides for alkali metal ions storage, ChemSusChem **13**, 1114 (2020).

[5] S. Ullah, P. A. Denis, and F. Sato, Monolayer boron-arsenide as a perfect anode for alkali-based batteries with large storage capacities and fast mobilities, Int J Quantum Chem. **119**, e25975 (2019).

[6] Z. Ali, T. Zhang, M. Asif, L. Zhao, Y. Yu, and Y. Hou, Transition metal chalcogenide anodes for sodium storage, Mater. Today, **35**, 131 (2020).

[7] K. S. Novoselov, A. K. Geim, S. V. Morozov, D. Jiang, Y. Zhang, S. V. Dubonos, I. V. Grigorieva, and A. A. Firsov, Electric field effect in atomically thin carbon films, Science **306**, 666 (2004).

[8] M. Debbichi, L. Debbichi, and S. Lebègue, Controlling the stability and the electronic structure of transition metal dichalcogenide single layer under chemical doping, Phys. Lett. A **383**, 2922 (2019).

[9] M. Debbichi, L. Debbichi, and S. Lebègue, Tuning the magnetic and electronic properties of monolayer chromium tritelluride through strain engineering, Phys. Lett. A **384**, 126684 (2020).

[10] T. Ayadi, L. Debbichi, M. Badawi, M. Said, D. Rocca, and S. Lebègue, An ab initio study of the electronic properties of the ferroelectric heterostructure In_2Se_3/Bi_2Se_3, Appl. Surf. Sci. **538**, 148066 (2021).

[11] L. Debbichi, O. Eriksson, and S. Lebègue, Two-dimensional indium selenides compounds: An ab initio study, J. Phys. Chem. Lett. **6**, 3098 (2015).

[12] Y. Bahari, B. Mortazavi, A. Rajabpour, X. Zhuang, and T. Rabczuk, Application of two-dimensional materials as anodes for rechargeable metal-ion batteries: A comprehensive perspective from density functional theory simulations, Energy Storage Mater. **35**, 203 (2021).

[13] B. Akgenc, Two-dimensional black arsenic for Li-ion battery applications: A DFT study, J Mater. Sci. **54**, 9543 (2019).

[14] F. Ersan, G. Gökoglu, and E. Aktürk, Adsorption and diffusion of Lithium on monolayer transition metal dichalcogenides ($MoS_{2(1-x)}Se_{2x}$) alloys, J. Phys. Chem. C **119**, 28648 (2015).

[15] T. Bo, P.-F. Liu, J. Xu, J. Zhang, Y. Chen, O. Eriksson, F. Wang, and B.-T. Wang, Hexagonal Ti_2B_2 monolayer: A promising anode material offering high rate capability for Li-ion and Na-ion batteries, Phys. Chem. Chem. Phys. **20**, 22168 (2018).

[16] A. Urban, D.-H. Seo, and G. Ceder, Computational understanding of Li-ion batteries, NPJ Comput Mater, **2**, 1126 (2016).

[17] X. Tang, X. Guo, W. Wu, and G. Wang, 2D metal carbides and nitrides (MXenes) as high-performance electrode materials for Lithium-based batteries, Adv. Energy Mater. **8**, 1801897 (2018).

[18] K. Fan, Y. Ying, X. Li, X. Luo, and H. Huang, Theoretical investigation of V_3C_2 MXene as prospective high-capacity anode material for Metal-Ion (Li, Na, K, and Ca) batteries, J. Phy. Chem. C **123**, 18207 (2019).

[19] Y. Xie, Y. Dall'Agnese, M. Naguib, Y. Gogotsi, M. W. Barsoum, H. L. Zhuang, and P. R. C. Kent, Prediction and characterization of MXene nanosheet anodes for Non-Lithium-Ion batteries, ACS Nano. **8**, 9606 (2014).

[20] P. Bhauriyal, A. Mahata, and B. Pathak, Hexagonal BC_3 electrode for a high-voltage Al-Ion battery, J. Phys. Chem. C **122**, 2481 (2018).

[21] L. Shao, X. Duan, Y. Li, Q. Yuan, H. Ye, and P. Ding, A new metallic In_3O_4 sheet as an anode material for Sodium-Ion batteries, J. Phys. Chem. C **123**, 30213 (2019).

[22] Y. Wang, N. Song, X. Song, T. Zhang, Q. Zhang, and M. Li, Metallic VO_2 monolayer as an anode material for Li, Na, K, Mg or Ca ion storage: A first-principle study, RSC Adv. **8**, 10848 (2018).

[23] L. Jingsha, G. Chunxian, and C. M. Li, Recent advances of two-dimensional (2D) MXenes and phosphorene for high-performance rechargeable batteries, ChemSusChem, **13**, 1047 (2020).

[24] E. Yang, H. Ji, and Y. Jung, Two-dimensional transition metal dichalcogenide monolayers as promising Sodium Ion battery Anodes, J. Phys. Chem. C **119**, 26374 (2015).

[25] V. Mehta, H. S. Saini, S. Srivastava, M. K. Kashyap, and K. Tankeshwar, S-functionalized Mo_2C monolayer as a novel electrode material in Li-Ion batteries, J. Phys. Chem. C **123**, 25052 (2019).

[26] Z. Wei, L. Wang, M. Zhuo, W. Ni, H. Wang, and J. Ma, Layered tin sulfide and selenide anode materials for Li- and Na-ion batteries, J. Mater. Chem. A **6**, 12185 (2018).

[27] W.-H. Lai, Y.-X. Wang, J.-Z. Wang, S.-L. Chou, and S.-X. Dou, Manipulating 2D few-layer metal sulfides as anode towards enhanced Sodium-Ion batteries, Batteries Supercaps **3**, 236 (2020).

[28] M. Zhang, H. Xie, H. Fan, T. Zeng, W. Yang, W. Zheng, H. Liang, and Z. Liu, Two-dimensional carbon-coated CoS_2 nanoplatelets issued from a novel $Co(OH)(OCH_3)$ precursor as anode materials for lithium ion batteries, Appl. Surf. Sci. **516**, 146133 (2021).

[29] Y. Dong, W. Shi, P. Lu, J. Qin, S. Zheng, B. Zhang, X. Bao, and Z. Wu, 2D holey cobalt sulfide nanosheets derived from metal–organic frameworks for high-rate sodium ion batteries with superior cyclability, J. Mater. Chem. A **6**, 14324 (2018).

[30] M. He, L. Zhu, Y. Liu, H. Wen, Y. Hu, and B. Li, Interfacial effect of Co_4S_3-Co_9S_8 nanoparticles hosted on rGO sheets derived from molecular precursor pyrolysis on enhancing electrochemical behaviour, Catal. Sci. Technol. **10**, 3622 (2020).

[31] M. Shi, Q. Wang, J. Hao, H. Min, H. You, X. liu, and H. Yang, MOF-derived hollow Co_4S_3/C nanosheet arrays grown on carbon cloth as the anode for high-performance Li-ion batteries, Dalton Trans. **49**, 14115 (2020).

[32] G. Zhou, H. Tian, Y. Jin, X. Tao, B. Liu, R. Zhang, Z. W. Seh, D. Zhuo, Y. Liu, J. Sun, J. Zhao, C. Zu, D. S. Wu, Q. Zhang, and Y. Cui, Catalytic oxidation of Li_2S on the surface of metal sulfides for Li-S batteries, PNAS **114**, 840 (2017).

[33] B. Xiao, Y.-c. Li, X.-f. Yu, and J.-B.bo Cheng, Pentagraphene: A promising anode material as the Li/Na-Ion battery with both extremely high theoretical capacity and fast charge/Discharge rate, ACS Appl. Mater. Interfaces **8**, 35342 (2016).

[34] P. Giannozzi *et al.*, QUANTUM ESPRESSO: A modular and open-source software project for quantum simulations of materials, J. Phys.: Condens. Matter **21**, 395502 (2009).

[35] P. E. Blöchl, Projector augmented-wave method, Phys. Rev. B **50**, 17953 (1994).

[36] J. P. Perdew, K. Burke, and M. Ernzerhof, Generalized Gradient Approximation Made Simple, Phys. Rev. Lett. **77**, 3865 (1996).

[37] H. J. Monkhorst and J. D. Pack, Special points for brillouin-zone integrations, Phys. Rev. B **13**, 5188 (1976).

[38] M. Cococcioni and S. de Gironcoli, Linear response approach to the calculation of the effective interaction parameters in the LDA+U method, Phys. Rev. B **71**, 035105 (2005).

[39] L. Liu, I. Kankam, and H. L. Zhuang, Single-layer antiferromagnetic semiconductor CoS_2 with pentagonal structure, Phys. Rev. B **98**, 205425 (2018).

[40] G. Henkelman, B. P. Uberuaga, and H. Jónsson, A climbing image nudged elastic band method for finding saddle points and minimum energy paths, J. Chem. Phys. **113**, 9901 (2000).

[41] W. Tang, E. Sanville, and G. Henkelman, A grid-based bader analysis algorithm without lattice bias, J. Phys.: Condens. Matter **21**, 084204 (2009).

[42] X. Zhang, L. Jin, X. Dai, G. Chen, and G. Liu, Two-dimensional GaN: An excellent electrode material providing fast Ion diffusion and high storage capacity for Li-Ion and Na-Ion batteries, ACS Appl. Mater. Interfaces **10**, 38978 (2018).

[43] W. Zhang, J. Yin, P. Zhang, X. Tang, and Y. Ding, Two-dimensional phosphorus carbide as a promising anode material for lithium-ion batteries, J. Mater. Chem. A, **6**, 12029 (2018).

[44] Y. Zhou, MX (M = Ge, Sn; X = S, Se) sheets: Theoretical prediction of new promising electrode materials for Li ion batteries, J. Mater. Chem. A, **4**, 10906 (2016).

[45] D. Wang, Y. Liu, X. Meng, Y. Wei, Y. Zhao, Q. Pang, and G. Chen, Two-dimensional VS_2 monolayers as potential anode materials for lithium-ion batteries and beyond: First-principles calculations, J. Mater. Chem. A **5**, 21370 (2017).

[46] S. Lei, X. Chen, B. Xiao, W. Zhang, and J. Liu, Excellent electrolyte wettability and high energy density of B_2S as a two-dimensional dirac anode for Non-Lithium-Ion batteries, ACS Appl. Mater. Interfaces **11**, 28830 (2019).

[47] X. Li, Q. Wang, and P. Jena, ψ-graphene: A new metallic allotrope of planar carbon with potential applications as anode materials for Lithium-Ion batteries, J. Phys. Chem. Lett. **8**, 3234 (2017).

[48] Y. Yu, Z. Guo, Q. Peng, J. Zhou, and Z. Sun, Novel two-dimensional molybdenum carbides as high capacity anodes for lithium/sodium-ion batteries, J. Mater. Chem. A **7**, 12145 (2019).

[49] X. Zhang, J. Hu, Y. Cheng, H. Y. Yang, Y. Yao, and S. A. Yang, Borophene as an extremely high capacity electrode material for Li-ion and Na-ion batteries, Nanoscale **8**, 15340 (2016).

[50] X. Zhang, Z. Yu, S. Wang, S. Guan, H. Yang, Y. Yao, and S. Yang, Theoretical prediction of MoN_2 monolayer as a high capacity electrode material for metal ion batteries, J. Mater. Chem. A **4**, 15224 (2016).

[51] F. Xiong and Y. Chen, A first-principles study of janus monolayer TiSSe and VSSe as anode materials in alkali metal ion batteries, Nanotechnology **32**, 025702 (2020).

[52] Y. Ding, B. Xiao, J. Li, Q. Deng, Y. Xu, H. Wang, and D. Rao, Improved transport properties and novel Li diffusion dynamics in van der waals C_2N/Graphene heterostructure as anode materials for Lithium-Ion batteries: A first-principles investigation, J. Phys. Chem.C **123**, 3353 (2019).

[53] A. Kokalj, Formation and structure of inhibitive molecular film of imidazole on iron surface, Corros Sci, **68**, 195 (2013).

[54] Y. Jing, J. Liu, Z. Zhou, J. Zhang, and Y. Li, Metallic Nb_2S_2C monolayer: A promising two-dimensional anode material for Metal-Ion batteries, J. Phys. Chem. C **123**, 26803 (2019).

[55] M. Debbichi and S. Lebègue, Crystal and electronic structures of nitridophosphate compounds as cathode materials for Na-ion batteries, Phys. Rev. B **92**, 085127 (2015).

[56] M. Debbichi, L. Debbichi, Van An Dinh, and S. Lebègue, First- principles study of the crystal, electronic structure, and diffusion mechanism of polaron-Na vacancy of $Na_3MnPO_4CO_3$ for Na-ion battery applications, Phys. D: Appl.Phys. **50**, 045502 (2017).

[57] N. Khossossi, V. Shukla, Y. Benhouria, I. Essaoudi, A. Ainane, R. Ahuja, G. Babu, and P. M. Ajayan, Exploring the possibility of β-Phase arsenic-phosphorus polymorph monolayer as anode materials for Sodium-Ion batteries, Adv. Theory Simul. **3**, 2000023 (2020).

[58] N. Yadav, B. Chakraborty, and T. J. Dhilip Kumar, First-principles design and investigation of siligraphene as a potential anode material for Na-Ion batteries, J. Phys. Chem. C **124**, 11293 (2020).

[59] B. Ball and P. Sarkar, Triazine- and keto-functionalized porous covalent organic framework as a promising anode material for Na-Ion batteries: A first-principles study, J. Phys. Chem. C **124**, 15870 (2020).

[60] M. Wu, B. Xin, W. Yang, B. Li, H. Dong, Y. Cheng, W. Wang, F. Lu, W.-H. Wang, and H. Liu, Metallic monolayer Ta_2CS_2: An anode candidate for Li^+, Na^+, K^+, and Ca^{2+} Ion batteries, ACS Appl. Energy Mater. **3**, 10695 (2020).

[61] Y. Zhoua and X. Zu, Mn_2C sheet as an electrode material for lithium-ion battery: A first-principles prediction, Electrochim. Acta **235**, 167 (2017).